Fuel 304 (2021) 121451

Contents lists available at ScienceDirect

Fuel

journal homepage: www.elsevier.com/locate/fuel

Full Length Article

Effect of calcium chloride on the self-ignition behaviours of coal using hot-plate test

Bei Li [a,b,*], Hong-peng Lv [a], Jun Deng [b,*], Li-li Ye [a], Wei Gao [a], Ming-shu Bi [a]

[a] School of Chemical Engineering, Dalian University of Technology, Dalian, Liaoning 116024, PR China
[b] State Key Laboratory of Coal Resources in Western China, Xi'an University of Science and Technology, Xi'an, Shaanxi 710054, PR China

ARTICLE INFO

Keywords:
Calcium chloride
Coal spontaneous combustion
Hot plate test
Thermogravimetric
Inhibition effect

ABSTRACT

The effect of calcium chloride ($CaCl_2$) on the self-ignition behaviours of coal was studied under air atmosphere in this paper. Aqueous $CaCl_2$ solutions (50, 100, 200, and 300 g/L) was used to treat a non-caking coal sample with high self-ignition potential, and the minimum auto-ignition temperature (MAIT) of the coal dust layer was determined using hot plate test to affirm thermal runaway. Both thermogravimetric analyzer and differential scanning calorimetry (TGA-DSC) were applied to investigate the decomposition of the samples. Results showed that $CaCl_2$ generated a coating film with dense slurry-like envelope on the particle surface, which took an inhibition effect at low thermal conditions (before crossing point) because of heat absorption of moisture evaporation and oxygen diffusion resistance of pore structure blockage. The MAIT of the $CaCl_2$-treated coal sample was increased from 210 to 240 °C, with a max elevation of 30 °C in comparison to H_2O-Coal sample. However, opposite effect was also found at higher temperatures (after the crossing point). For 50 g/L $CaCl_2$-Coal sample on hot surface of 240 °C, the calculated inhibiting rate at 10 and 50 min was 54.8% and −115.6%, respectively, suggesting that the catalysis effect at the later stage after ignition was over two times than the inhibiting effect at the initial self-ignition process. The Ca^{2+} in the form of its oxides (CaO and CaO_2) at higher thermal conditions promoted the diffusion of oxygen to the coal surface and expanded the main combustion zone, suggesting a catalytic role in the coal combustion.

1. Introduction

Coal spontaneous combustion (CSC) is an objective phenomenon in nature, which has existed for millions of years in the Earth's history [1]. It is the most common cause that triggers surface and subsurface coal fires by self-ignition. Globally, the hot spot of coal fire cases reported in publications [2–5] due to CSC come from the US, India, China, as well as other major coal mining countries like Australia, Spain, Poland, and Czech Republic. The coal-bed fires in Powder River Basin (PRB) region in the US had started naturally>4 million years [1,2]. The uncontrollable coal fires in Jharia Coalfield (JCF) in India burned from early 1900s [6]. It's generally approved that self-heating of coal was due to the reactions of oxygen-containing group on coal surface with oxygen in the air, and the heat releasing from oxidation reactions directly caused the increase in temperature. As reported by Song et al. [7], the thermal energy release of long flame coal during a low temperature oxidation condition was 1648.0 J/g at the accelerating exothermic stage (from 69.4 to 145.8 °C) and 4134.7 J/g at the quick exothermic stage (from 145.8 to 200 °C) respectively. Therefore, CSC occurred when the coal temperature exceeded a critical value (almost ~ 80 °C). Then smoldering combustion of coal developed at a low propagation rate without flame until the ignition point reached. In general, the coal fire caused by CSC had the following risks and potential hazards [2,7–10]: (i) resource ruin. A huge of coal resources were burnt out due to the coal wildfires, e.g., the untapped coal resource relating to areas nearly 5 km^2 of 18 fire zones were locked in underground and attacked by wildfires in Wuda Coalfield of northern China [8], (ii) environmental pollution. Numerous toxic and harmful gases (such as CO, SO_2, and NOx) produced through CSC [9] aggravated the climate warming. Emissions from continuous burning coal fires slowed down the action plan for peaking carbon dioxide emissions before 2030 and conflicted with the goal of carbon neutralization before 2060 in China, (iii) casualty accident initiator. >90% of coal fire incidents in the goaf areas occurred and resulted from CSC [2]. A fatal gas explosion of Babao coal mine (Jilin Province, China) caused 36 deaths on March 29, 2013 and the ignition source of the accident was attributed to CSC in the mined-out area known as the goaf [10]. Therefore, the investigation on CSC prevention remains a hot topic

* Corresponding authors at: School of Chemical Engineering, Dalian University of Technology, Dalian 116024, PR China (B. Li).
E-mail addresses: libei422@dlut.edu.cn (B. Li), dengj518@xust.edu.cn (J. Deng).

https://doi.org/10.1016/j.fuel.2021.121451
Received 6 February 2021; Received in revised form 3 June 2021; Accepted 13 July 2021

Nomenclature

d	Diameter, mm
$DTG_{min\text{-}I}$	Peak mass loss rate in stage I, %/°C
$DTG_{max\text{-}III}$	Peak mass loss rate in stage III, %/°C
I_T	Inhibiting rate, %
L	Height, mm
R	Correlation coefficient
q	Heat flow per gram of sample, W/g
Q_o	Heat released per gram of coal sample mass, kJ/g
ΔQ	Sum of the heat released from coal at corresponding stage, kJ/g
ΔS	Area obtained by integration of DSC in the temperature interval, J
T_{cp}	Temperature at the crossing point, °C
T_p	Temperature of the hot plate, °C
T_{max}	Maximum temperature in the layer, °C
$T_{min\text{-}I}$	Temperature at minimal mass of moisture evaporation, °C
$T_{max\text{-}II}$	Temperature at the maximum mass increase, °C
$T_{max\text{-}III}$	Temperature at the maximum mass loss rate in stage III, °C
t_1	1st inflection time, min
t_2	2nd inflection time, min
t_{id}	Ignition delay time, min
t_{cp}	Time at the crossing point, min
t_{max}	Time at which maximum temperature reached, min
$t_{min\text{-}I}$	Time at the temperature of $T_{min\text{-}I}$, s
$t_{max\text{-}II}$	Time at the temperature of $T_{max\text{-}II}$, s
$W_{\text{-}I}$	Weight loss at the minimal mass of moisture evaporation in stage I, %
$W_{\text{-}II}$	Mass increase in stage II, %

Greek symbols

β	heating rate, °C/min

Abbreviations

CSC	Coal spontaneous combustion
CPT	Crossing point temperature, °C
DSC	Differential scanning calorimetry
JCF	Jharia Coalfield
MAIT	Minimum auto-ignition temperature, °C
PRB	Powder River basin
PSD	Particle size distribution
pH	Pondus hydrogenii
SEM	Scanning electron microscope
TGA	Thermogravimetric analysis

in present.

Utilization of inhibitor is one of the most effective methods to prevent CSC [11–13]. Fig. 1 displays a principle of perfusion system through high-pressure rubber hose, which could configure and convey a desired concentration of inhibitor slurry for extinguishing coal fires at surface and underground goaf [14,15]. Because of non-toxic in nature, cheapness in purchase, and convenient in storage and transportation, the resistance agents of inorganic salt (the calcium chloride, $CaCl_2$) is widely used for CSC prevention and coal fire extinguishing engineering. For example, a successful application case reported in Huasheng coal mine (Shanxi Province, China) [16] showed that $CaCl_2$ had a well inhibition effect on CSC prevention in underground. The slurry configured by 20% $CaCl_2$ solution was sprayed in the areas of hydraulic supports and goaf at regular intervals, achieving well effect on avoiding the CSC incidents at these areas. In addition, another field application of fire retardants of $CaCl_2$ and $MgCl_2$ with H_2O at a ratio of 1:1:10 was reported in India to extinguish the overburden coal fire zones in Shatbadi opencast [17]. The field experiments manifested that the temperature of an area of 100 m^2 was decreased from 450 to 92 °C, resulting well efficacy for coal fire control. The indicators of the $CaCl_2$-treated coal sample, such as weight change, critical decomposition temperature, released heat, gaseous product, and kinetic parameter are commonly examined

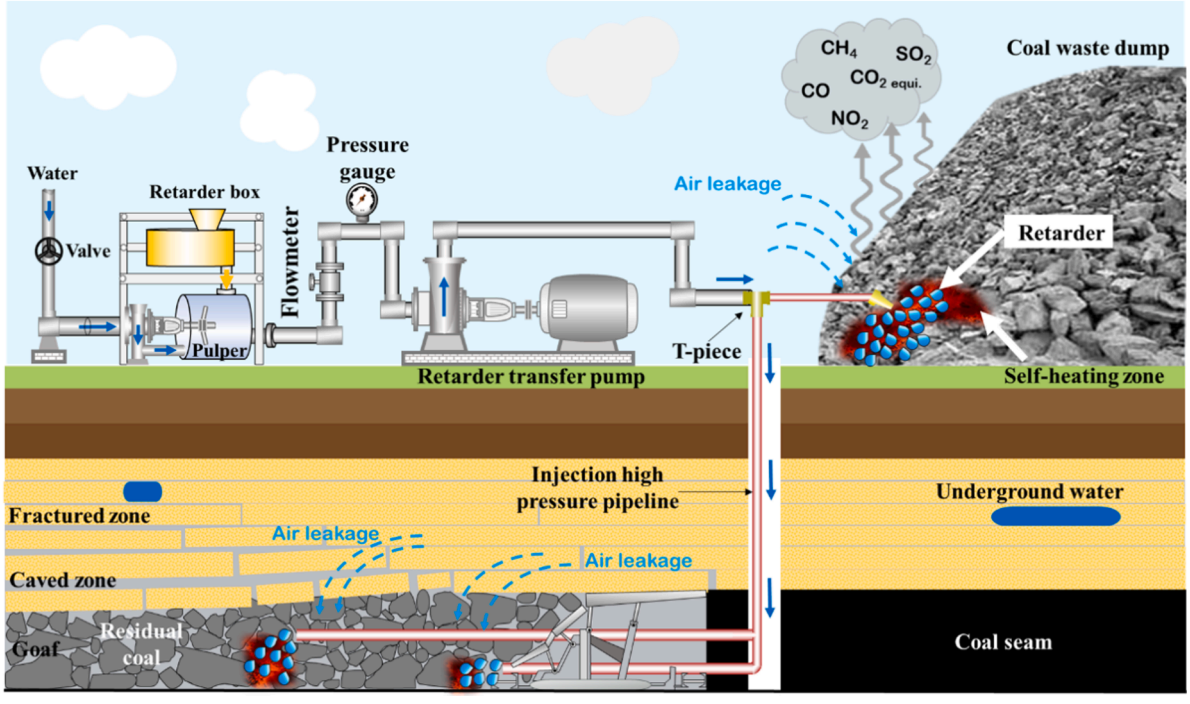

Fig. 1. Perfusion system of the inhibitor for prevention of coal fire hazards.

to evaluate the inhibition performance during coal combustion and pyrolysis process. Studies [12,17,20,21,23,26,27] of the effectiveness of $CaCl_2$ and other inorganic additives during the combustion and pyrolysis of coal are tabulated in Table 1. Tang et al. [18] declared that the oxidation of methyl, methylene, methine, and hydroxy groups could be inhibited by inorganic chloride below 200 °C. This was because the generated Cl* reacted with combustible materials instead of considerable amounts of OH*, H*, and O* so that it inhibited the CSC. Higher gaseous yields means that the coal is oxidized more violently under the same experimental conditions [19]. Cui et al. [20] investigated five thermo-responsive inhibitors including $CaCl_2{\cdot}6H_2O$. They used inhibiting rate based upon the CO emission to evaluate the effect of additive to coal. Their results showed a maximum inhibiting rate of $CaCl_2{\cdot}6H_2O$ was 79.9% at 171.8 °C. A designed temperature-programmed system by Wu et al. [12] found that the CO production from the 20% $CaCl_2$-treated coal sample was less than that of the 20% $MgCl_2$-treated coal sample during low-temperature oxidation (20–200 °C), showing that $CaCl_2$ solution had better suppression on CSC. However, they did not make further analysis and explanation on the inhibition mechanism of $CaCl_2$. Minerals containing Ca^{2+} was studied by Wang et al. [21] to explore the oxy-enriched combustion reactivity and kinetics of Zhundong coal in atmosphere of 30% O_2/70% CO_2. They illustrated that the $CaCl_2$ had reduced the average combustion rate of coal from 4.44 to 3.83%/°C as well as prolonged the corresponding combustion time under the same thermal conditions. The burnout temperature shifted to right and the main temperature zone (from ignition temperature to burnout temperature) was expanded with combustion time increasing. However, Pan [22] pointed out that $CaCl_2$ had clearly promoting effect on shifting the main reaction zone (400–500 °C) to higher temperatures. Another study from Sunel et al. [23] using a fixed-bed tube furnace indicated that Ca^{2+} could enhance the production of CO_2 and CH_4 at temperature range from 800 to 1200 °C in nitrogen atmosphere, suggesting a promoting effect on coal combustion at higher temperature stage.

Thermal runaway is a vital phenomenon in understanding the transformation of coal fire from CSC. The standard of IEC 60079–14–2013 recommended a procedure for evaluation of thermal runaway ability of self-heating substances. The thermal sensibility of the substance to occur CSC is accessed by exposure of it to air atmosphere at a hot surface at a certain temperature. Classification of a self-heating substance is determined by the critical surface temperature that drives a sustained thermal runaway. Resent years, the ignition properties of solid fuels were measured by hot plate method to evaluate their thermal susceptibility [24,25]. The minimum auto-ignition temperature (MAIT) represents the lowest initial temperature that leads to a sustained exothermic reaction, and can be used to evaluate the coal sample's self-ignition sensibility. As can be seen in Table 1, thermal analysis techniques such as thermogravimetric analysis (TGA), and differential scanning calorimetry (DSC) in present studies [17,20,21,26] were commonly used to investigate the effectiveness of inorganic additives during the combustion and pyrolysis of coal. However, the influence of $CaCl_2$ on the ignition properties of coal is seldom studied by using the hot plate apparatus. The generation of self-ignition source of coal treated with additives at different thermal conditions gets little attention. Parameters required for determining ignition properties such as the ignition delay time (t_d) of $CaCl_2$ treated coal are rarely known or investigated. These parameters are crucial because it can give instructions to field projects, knowing the emergence response time for the control of coal fire [13]. Therefore, it is benefit for investigating the effects of calcium chloride addition on the self-ignition behaviours of coal during the whole process of CSC.

In present work, the smoldering process of the coal samples were investigated by using hot plate test to explore their ignition characteristics, such as the maximum temperature in the layer (T_{max}), the MAIT, and t_d. In addition, thermal analysis (TGA–DSC) was applied to characterise the weight and pronounced heat evolution of the samples during CSC process. The self-ignition behaviours of the $CaCl_2$ solution treated coal sample at various concentration was determined and compared to a coal-water blank sample to analyse the inhibitory effect of the additives. The research of this work would provide potential engineering guidance for safety engineers to use calcium chloride additive in CSC prevention and coal fire elimination applications.

Table 1
Summary of inorganic additives on coal pyrolysis and combustion.

Additive	Sample	Method	Atmosphere	Parameter	Heating rate (°C/min)	Temperature range (°C)	Author
Sodium element (NaCl, $NaCO_3$, $NaAlSi_3O_8$), calcium ($CaCl_2$, $CaCO_3$, $CaSO_4$), and iron (Fe_2O_3, Fe_3O_4, and FeS_2)	Coal from Zhundong mine, China; Synthetic coal	TG	30% O_2/70% CO_2	Combustion behaviours including temperature, weight change, and activation energy	0.01–100	30–1300	Wang et al., 2020 [21]
$CaCl_2$, KCl, $MnCl_2$, $ZnCl_2$, $NiCl_2$	Lignite coal	Fixed-bed tube furnace, flow drop-tube furnace, and FTIR	Nitrogen	Pyrolysis behaviours including gas production (CO_2, CO, CH_4, H_2), and functional group	–	800–1200	Sunel et al., 2019 [23]
$CaCl_2$, Na_2CO_3, $NaHCO_3$, $Co(NO_3)_2$, H_2O_2, procyanidine, attapulgite clay	Zhundong coal, Shendong coal, and Pingshuo coal, China	Crossing point temperature (CPT) (i), TGA-DSC (ii), FTIR (iii)	Air	Spontaneous combustion properties including CO, O_2, weight change, released heat, temperature, and functional group	0.8 (i), 2 (ii), 1 (iii)	40–70 (i), 30–800 (ii), and 30–220 (iii)	Zhong et al., 2018 [26]
$CaCl_2$, $MgCl_2$, and sodium bicarbonate	Coal from Datun mine	Temperature-programmed system	Nitrogen	Spontaneous combustion properties including CO, O_2, weight change, and temperature	1	20–200	Wu et al., 2018 [12]
$CaCl_2$, $MgCl_2$, $NaHCO_3$, $Na_2S_2O_3$, and $CO(NH_2)_2$	Coal from Longdong Mine, China	Temperature-programmed system (i), DSC (ii), TG-DTG-DSC (iii)	Air	Spontaneous combustion properties including gas production (CO, O_2), weight change, released heat, inhibitor rate based upon CO	1 (ii), 2 (i), and 10 (iii)	30–200 (i, ii), 30–800 (iii)	Cui et al., 2018 [20]
$CaCl_2$, NaCl, K_2SO_4, $MgCl_2$	Coal from India	CPT (i), DSC (ii)	Oxygen	Spontaneous combustion properties including temperature, and released heat	1 (i), 10 (ii)	<174 (i), 30–600 (ii)	Pandey et al., 2015 [17]
$CaCl_2$ and urea	Bituminous coal	TGA-DSC	Oxygen	Low-temperature oxidation properties including temperature, weight change, released heat, and activation energy	2, 5, 10, and 20	30–300	Václav Slovák, et al., 2012 [27]

2. Experiment

2.1. Preparation of calcium chloride-loaded coal sample

Low metamorphic coal is prone to emerge spontaneous combustion due to self-heating. A non-caking coal with higher-combustible contents was gleaned from Daliuta Coal Mine in north of China. The fresh coal lump was milled after it was delivered to the laboratory. The $CaCl_2$ was selected as the additive for three reasons: (i) it has non-toxic in nature and soluble in water, (ii) it can be accessed widely in inexpensive way, and (iii) it has been verified to possess effectiveness at suppressing spontaneous coal combustion [28] and coal dust explosions [22] in engineering practice. The $CaCl_2$ was provided by Xilong Scientific Co., Ltd. (Shantou, Guangdong, China) and applied to obtain calcium chloride-loaded coal ($CaCl_2$-Coal) samples in this study. Aqueous additive solution at various concentrations of 50, 100, 200, and 300 g/L were prepared by dissolving appropriate amount of $CaCl_2$ to deionised water. For investigating the effect of $CaCl_2$ on self-ignition behaviours of coal, 50 mL of the additive solution was added into 110 g of coal dust samples to form a $CaCl_2$-Coal dispersion. To exclude the effect of water on the micro-structure of coal when the sample treated with aqueous solution, the water-treated coal (H_2O-Coal) following the same procedure was used as the black sample for comparative study with the additive treated coal. The samples were then dried in air flow with duration of 48 h at 30 °C.

2.2. Sample characterization

The basic physical and chemical properties of the $CaCl_2$-Coal samples were systematically measured and studied in present work. The particle size distribution (PSD) of the dust samples were subjected using a Malvern laser particle size analyzer (Model Mastersizer 2000, Malvern Instruments Ltd., Malvern, UK). A tungsten lamp scanning electron microscope (SEM, Model Quanta 450, FEI, Hillsboro, USA) was used to scan the the surface morphology and porosity of the prepared samples at 3000 and 5000 times of micro-magnification. The pondus hydrogenii (pH) value of the $CaCl_2$-Coal solutions was determined using a pH meter (Testo 206pH2, Testo Instruments International Trading Ltd., Shanghai, China) during coal sample preparation. Each prepared $CaCl_2$-Coal solution at particular concentration was tested in triplicate.

2.3. Hot plate test apparatuses

The effectiveness of additive on retarding ignition properties of pulverized coal dust layer are estimated on a hot plate test apparatus. On basis of the experimental system shows in Fig. 2, the hot plate test device is designed to measure the ignition characteristic parameters. The surface temperature of the plate (area of hot surface 200 × 200 mm^2) controlled by a temperature regulator provides a constant heating temperature with a thermometric error of ± 3 °C. A stainless ring (10-mm in height [L] and 100-mm in diameter [d]) for the holding prepared samples was located at the geometric center of the plate. Four K-type thermocouples were placed at the inter-space centre of the ring at height of 2.5, 4.5, 7.2, and 9.0 mm above the upper surface of the plate. The experimental procedure and ignition criterion are followed by previous study in ref. [24,25].

2.4. Thermal analysis apparatuses

Simultaneous thermal analysis of the sample was performed using a SDT-Q600 analyzer (TA Instruments, New Castle, Pennsylvania, USA) to obtain the thermogravimetric (TG), differential scanning calorimetry (DSC), and their differential values (denoted as DTG). Approximately 20 mg of the dry sample was taken and placed in the sample crucible for each test. High degree of standard air (oxygen 21 vol%) was employed as the reaction gas environment at a flow rate of 50 mL/min. Heating rate is a vital factor that would affect the decomposition process of solid fuel. The peak temperature during the chemisorption stage of coal oxidation shift rightward with increasing heating rate [29]. The coal sample would be subjected adequate oxidation and pyrolysis at low heating rate [27]. Therefore, a heating rate of 10 °C min^{-1} was selected in present study for thermal treatment of the sample at a heating temperature range from 30 to 800 °C. Each analysis was performed at least twice to ensure the accuracy and stability.

3. Results and discussion

3.1. Characterization of the prepared sample

The definition of coal dust size was dated to the term “mine size coal” adopted in Bureau of Mines Technical Paper (TP) 464 [30]. TP 464 stated that all coal dust passing a US Standard 20-mesh sieve (850 μm) meanwhile of which 20% having through a 200-mesh sieve (75 μm) could be considered to be typical “mine size dust” [31]. PSD results [25] shown that the maximum particle size of prepared coal sample was 478 μm, while particle size d_{90} was 289 μm. In addition, the accumulative volume of particle size <75 μm had a proportion of 36%, indicating the prepared coal dust was within the available size range of the “mine-dust”. Material properties of the coal sample are listed in Table 2.

The pH value of the $CaCl_2$-Coal solution with various consecrations at room temperature are depicted in Fig. 3d. As a strong acid weak base salt, $CaCl_2$ is highly hygroscopic and easily soluble in water (slightly

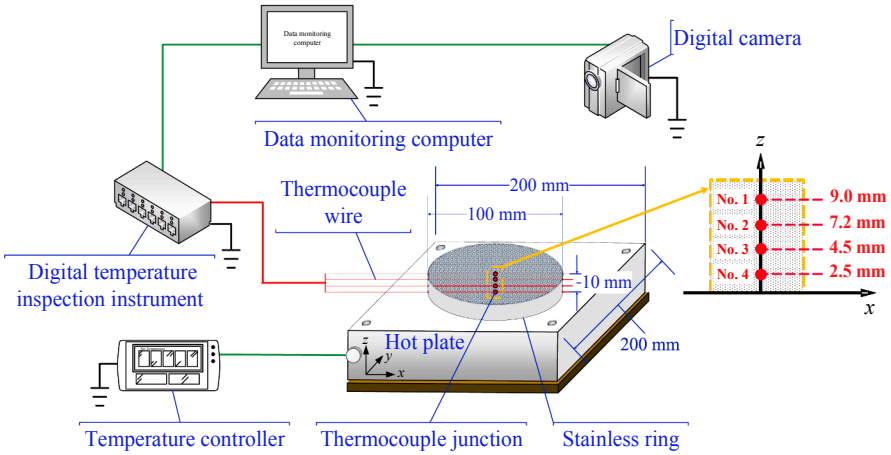

Fig. 2. Schematic of the test apparatuses measuring coal dust layer ignition properties.

Table 2
Material properties of the Daliuta coal sample.

Proximate analysis, wt% (air-dry basis) [25]				
Moisture	Ash	Volatiles	Fixed carbon	
10.7	5.3	27.6	56.4	
Ultimate analysis, wt% (dry ash-free basis) [25], * by difference method according to ISO17247-2013				
Carbon	Hydrogen	Nitrogen	Total Sulfur	Oxygen*
71.6	4.1	0.8	0.2	7.3
$CaCl_2$-to-Coal mass ratio, %				
Sample	50 g/L $CaCl_2$-Coal	100 g/L $CaCl_2$-Coal	200 g/L $CaCl_2$-Coal	300 g/L $CaCl_2$-Coal
Mass ratio	0.73	1.45	2.90	4.36

acidic). The solution of $CaCl_2$ becomes acidic when dissolved in water. The pH of the $CaCl_2$-Coal solution was in a range of 5.29–5.01, which decreased as the mass concentration of $CaCl_2$ increased. The solution of raw coal treated with water has a pH value of 6.38 ± 0.21 which is the background value in present study. The calculated mass ratio of $CaCl_2$–to–Coal at various concentrations was in a range of 0.73%–4.36%. The SEM images of the raw coal and the calcium chloride-loaded coal samples are presented in Fig. 3. As showed in Fig. 3b–c, the micro surface morphology of the raw coal sample exhibited matrix porosity and fractures with its unique structure and clear outline. However, a coating film with dense slurry-like envelope is formed on the surface of the $CaCl_2$-Coal sample (Fig. 3e–f), on which visible crystal particles of calcium chloride can be scanned.

3.2. Critical hot surface temperature of coal dust accumulation

Thermal runaway happened inside the coal dust layer when it contacted with a hot surface of the industrial equipment which reached at the MAIT point. The spontaneous exothermic reactions accelerated with a subsequent chemical heat release [32]. Subsequently, the self-ignition process became chemical control model (exothermic oxidation reaction) from physical control mode (heat conduction), which caused a fast-increasing temperature change in the inner layer [33]. According to our previous study [25], measuring point no. 2 was the optimal ignition position in the pulverized coal dust layer in consideration of oxygen diffusion resistance and heat losses of upper surface of dust layer. Therefore, the temperature at measuring point no. 2 (7.2 mm away from the hot surface) was selected among the four thermocouples to represent the typical temperature–time history of the layer. As can be seen in Fig. 4a, non-ignition occurred at the hot surface temperature of 200 °C. However, an inflammable point took place and plenty of cracks appeared on the surface of the coal dust layer at 210 °C. Correspondingly, temperature evolution of coal layer at critical condition of ignition in Fig. 4b showed obvious difference with that of the non-ignition case. The MAIT of H_2O-Coal sample was taken as 210 °C. The definition of ignition delay time (t_{id}) followed by Joshi et al. [32] which are the time interval from the start of sample heating to the middle of rapid temperature rise. Moreover, the determination methods of the 1st inflection time (t_1) and 2nd inflection time (t_2) from temperature records obeyed the rules by Wu et al. in ref. [34]. Based upon the results from Fig. 4b and c, the t_1, t_2, and t_{id} of the H_2O-Coal sample were 25.5, 28.6, and 33.6 min, respectively. In addition, the T_{max} of the H_2O-Coal sample layer could reach 380.8 °C. Miao et al.'s [35] study on combustion characteristics of coal declared that the high-volatile coal (>10%) would show a phenomenon of separated combustion phenomenon of volatile matter and char combustion at certain oxygen conditions. As can be seen in Fig. 4c, the increase of temperature change rate at 21 and 45 min were attribute to the ignition of volatile and char respectively. When the initial hot surface temperature reached at MAIT, the volatile matter that released out through volatilization is ignited, so the temperature of the coal layer increased quickly due to violent oxidation reactivity. As the development of combustion process, the heat accumulated in the coal layer brought about the increase of char temperature and triggered the char combustion [36].

3.3. Effect of $CaCl_2$ on ignition properties of coal dust accumulation

Temperature evolution for the coal sample treated with $CaCl_2$ solution at various hot surface temperature are exhibited in Fig. 5. For the coal sample treated with 50 g/L $CaCl_2$ solution, a thermal runaway occurred in the dust accumulation at a hot surface temperature of

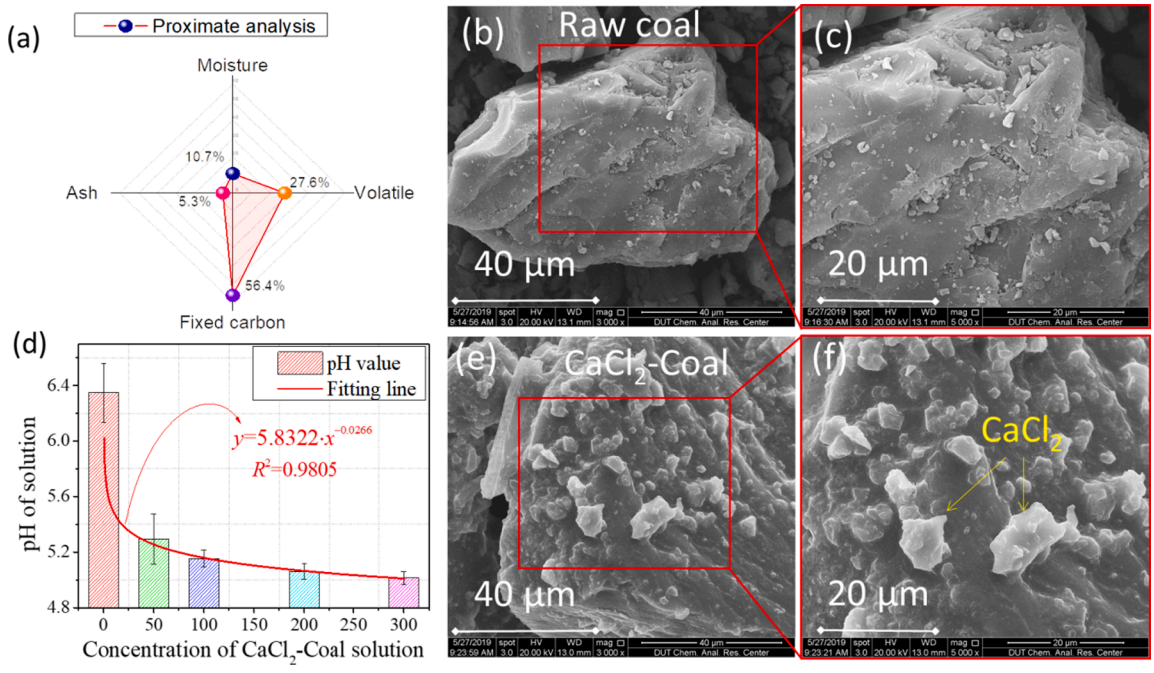

Fig. 3. Characterization of the prepared sample, (a) proximate analysis of the raw coal, (b) and (c) SEM images of the raw coal sample, (d) pH values of the $CaCl_2$-Coal solutions, (e) and (f) morphology of the $CaCl_2$ loaded coal sample.

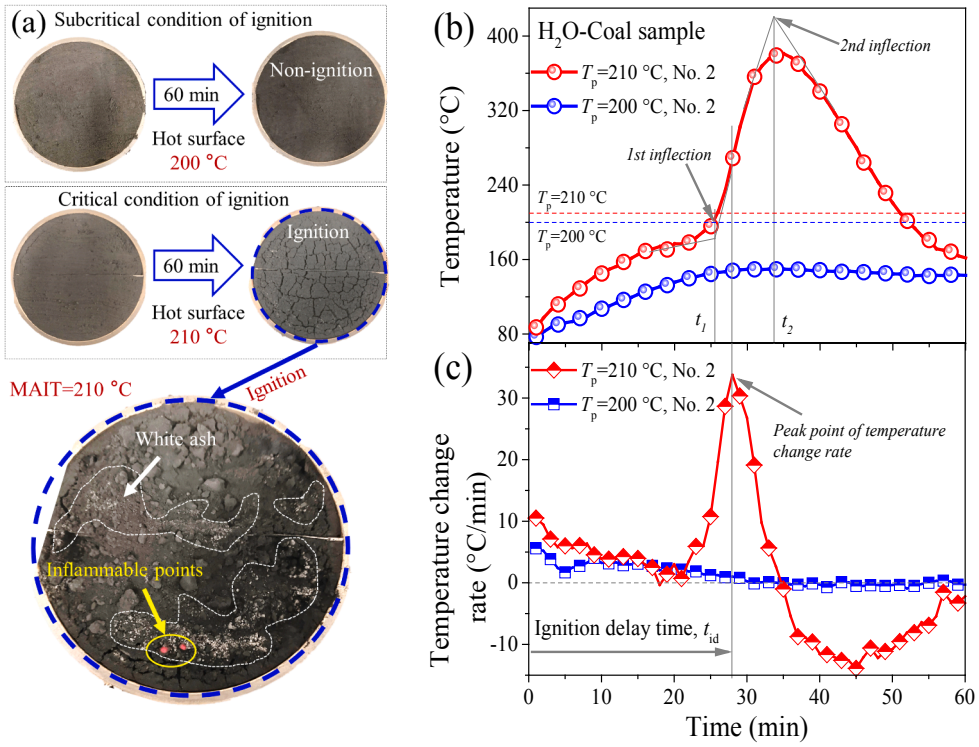

Fig. 4. Spontaneous combustion of water washed coal sample layer (black test), (a) surface morphology, an ignition occurred at critical condition, (b) temperature history of measuring point no. 2 at the coal dust layer under critical (T_p = 210 °C) and subcritical (T_p = 200 °C) conditions, and (c) their temperature change rates.

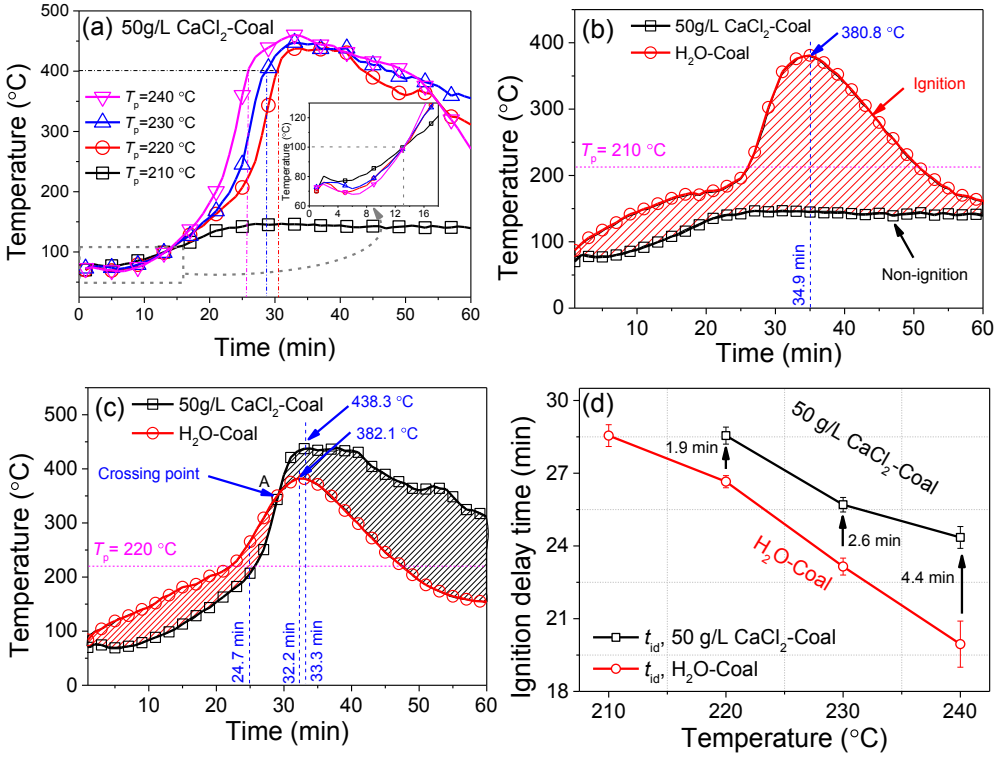

Fig. 5. Typical plots of temperature evolution for (a) 50 g/L $CaCl_2$-Coal sample on hot surface at various temperature, (b) samples at hot surface of 210 °C, and (c) samples at hot surface of 220 °C, and (d) ignition delay times.

220 °C. At the initial 13 min of heating process in Fig. 5a, the temperatures of the $CaCl_2$-treated coal samples at the ignition cases (T_p = 220, 230, and 240 °C) were lower than that of the non-ignition case (T_p = 210 °C). It was because higher thermal conditions caused more quickly water evaporation rate at this stage (<100 °C). In consequence, it absorbed more heat that made a lower temperature in the tested coal

dust layer. At the later self-heating process (>13 min), the chemisorption of oxygen began to strengthen. The exothermic reactions enhanced as the hot surface temperature elevated, so the temperature rise rate of coal was accelerated which led to the temperature curve of the dust layer at ignition cases shifted to left. At a hot surface of 210 °C in Fig. 5b, a fast-rising temperature change for the H_2O-Coal sample was caused by exothermic reactions and the peak temperature reached 380.8 °C at 34.8 min. Therefore, non-ignition for the 50 g/L $CaCl_2$-Coal appeared but the ignition happened for the H_2O-Coal sample. The critical hot surface temperature of 50 g/L $CaCl_2$-Coal on a hot surface was 10 °C higher than that of the H_2O-Coal sample. It means that the risk of CSC in terms of dust accumulation is reduced to some extent when the coal was treated with $CaCl_2$ solution.

To further illustrate the self-ignition behaviours, the temperature evolution of both coal sample treated with 50 g/L $CaCl_2$ and H_2O at thermal runaway condition (T_p = 220 °C) are depicted in Fig. 5c. The morphology with EDS mapping of the samples are demonstrated in Fig. S1. As can be seen in Fig. 5c, a crossing point (A) at 29.1 min was observed where the temperature of 50 g/L $CaCl_2$-Coal began to exceed the temperature of H_2O-Coal. The temperature and the correspondingly time at this crossing point (A) are marked T_{cp} and t_{cp} respectively. The results indicated that the treatment of $CaCl_2$ solution to coal inhibited the self-ignition process at the initial duration of 29.1 min until it reached T_{cp} (353.2 °C). However, at the later duration after the crossing point (A) of 353.2 °C, the temperature of $CaCl_2$-Coal sample layer was improved and reached its peak at 438.8 °C due to more intense oxidative decomposition of coal than that of H_2O-Coal sample. Previously studies [37,38] suggested that some of the carboxyl groups of calcium-loaded lignites decompose thermally between 200 and 700 °C and the carbon dioxide yield rate reached it peak at ~ 400 °C. In addition, Clemens et al. [39] indicated that a sufficient quantity of ion-exchanged calcium showed catalysis effect for improving the char consumption rate when it converted into distributed oxide crystallites on the char surface. The addition of $CaCl_2$ at higher temperature ($>T_{cp}$) enhanced the temperature of the coal dust layer when compared with the blank sample (H_2O-Coal), showing an impact of catalysis on the coal. These results were in consistent with Pan's results [22] in which he indicated that the existing of calcium in a higher temperature oxidizing environment would promoted coal decomposition and dominantly manifested as catalytic effect. According to the results in Fig. 5d, the ignition delay time of the 50 g/L $CaCl_2$-Coal sample was improved at least 1.9 min in the experimental condition. Detailed information of the characteristic parameters of ignition properties of coal dust accumulation at various thermal conditions are listed in Table 3.

3.4. Evaluation of suppressing effectiveness on coal with $CaCl_2$ treated

Temperature is a direct parameter to characterize the thermal state of coal accumulation during its self-heating process. To quantitatively study the effectiveness of the addition agent on various hot surface temperature, the inhibiting rate of $CaCl_2$ on coal was evaluated by a dimensionless index I_T based upon each temperature of the sample as written in Eq. (1).

$$I_T = \frac{T_{H_2O-Coal,T_p} - T_{CaCl_2\ -\ Coal,T_p}}{T_{H_2O-Coal,T_p}} \cdot 100\% \quad (1)$$

where I_T is the inhibiting rate, $T_{H_2O-Coal,T_p}$ and $T_{CaCl_2\ -\ Coal,T_p}$ are the temperature of $CaCl_2$-Coal and H_2O-Coal samples at hot surface temperature of T_p, respectively. Therefore, the inhibiting rates of 50 g/L $CaCl_2$-Coal sample at hot surface temperature from 210 to 240 °C are presented in Fig. 6.

The inhibiting rate of 50 g/L $CaCl_2$ at hot surface temperature of 210 °C showed two main peaks in the experimental duration. The first maximum inhibiting rate (39.8%) appeared at a temperature of 81.7 °C around 8 min, and then the second maximum inhibiting rate (61.9%) was at a temperature of 144.8 °C around 35 min. It clearly manifested that the sample treated with 50 g/L calcium chloride solution suppressed coal decomposition at hot surface temperature of 210 °C, indicating that the calcium chloride played an inhibition effect on CSC in whole experiment period. However, for the hot surface temperature of 220–240 °C, the effect of calcium chloride on coal was changed from inhibition to catalysis at crossing points of 29.7, 28.6, and 26.1 min, respectively. After the crossing point, the catalysis effect for coal combustion increased with time growing until they reached their maximum of 112.9%–115.6%. Take the 50 g/L $CaCl_2$-Coal sample on hot surface temperature of 240 °C for example, the inhibiting rates at 10 and 50 min were 54.8% and –115.6%, respectively, indicating that the catalysis effect at the later stage after ignition was over two times than the inhibiting effect at the initial self-ignition process.

3.5. Effect of $CaCl_2$ concentration on critical hot surface temperature

Fig. 7 shows the MAIT of the coal samples treated with various $CaCl_2$ concentrations. The MAIT of the sample increased from 210 to 240 °C with $CaCl_2$ concentrations increasing. The linear regression equation of MAIT has a high correlation coefficient (R^2) of 0.9956. For the coal sample treated with $CaCl_2$ solution, the dust accumulation on a hot

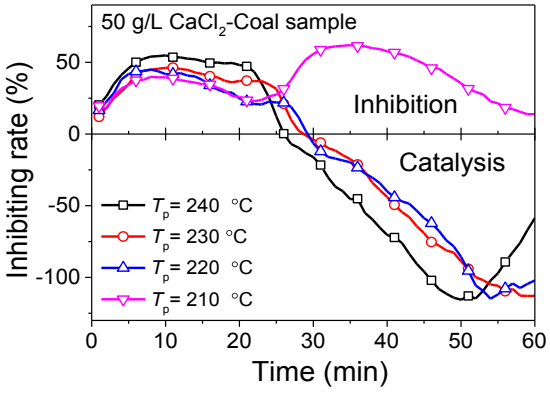

Fig. 6. Inhibiting rate of $CaCl_2$ treated coal samples (50 g/L $CaCl_2$-Coal) on hot surface at T_p ranged from 210 to 240 °C.

Table 3
Characteristic parameters of $CaCl_2$ treated coal sample at various hot surface temperatures.

T_p (°C)	Sample	State	t_1 (min)	t_{id} (min)	t_2 (min)	t_{cp} (min)	T_{cp} (°C)	T_{max} (°C)
240	50 g/L $CaCl_2$-Coal	Ignition	20.8	24.4	27.8	26.1	405.1	460.5
	H_2O-Coal	Ignition	15.2	20.0	24.6			410.1
230	50 g/L $CaCl_2$-Coal	Ignition	24.1	25.7	29.9	28.6	402	447.7
	H_2O-Coal	Ignition	18.5	23.2	29.2			400.8
220	50 g/L $CaCl_2$-Coal	Ignition	26.2	28.6	32.0	29.1	353.2	427.5
	H_2O-Coal	Ignition	22.9	26.7	32.8			381.9
210	50 g/L $CaCl_2$-Coal	Non-ignition	–	–	24.6	–	–	146.3
	H_2O-Coal	Ignition	25.2	28.6	34.8			380.8

Note: T_{cp} and t_{cp} are the temperature of the crossing point and its correspondingly time.

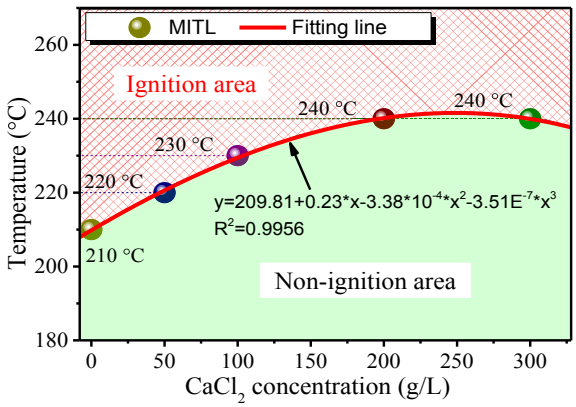

Fig. 7. MAIT of the $CaCl_2$ treated coal samples with various concentrations.

surface could not appear thermal runaway or self-ignition if the temperature was controlled under the MAIT (green area in Fig. 7). The emergence of the ignition in the coal dust layer was controlled by several factors, such as the thickness of layer, concentration of calcium chloride solution, and hot surface temperature. In present study, both 200 g/L $CaCl_2$-Coal and 300 g/L $CaCl_2$-Coal samples had the same MAIT of 240 °C, which was improved by 30 °C in comparison to H_2O-Coal sample. It clearly shown that the inhibitory effect on the coal was not increasing when the concentration of calcium chloride solution exceeds 200 g/L, suggesting that the $CaCl_2$ may have a critical value on inhibiting the self-ignition of coal. This was possible that the dense coating on the particle surface of the 300 g/L $CaCl_2$-Coal sample contracted and ruptured due to dehydration under the thermal environment (T_p = 240 °C). The degradation of the surface coating lead to an invalidation of blocking effect (Fig. S1d), which promoted the diffusion of oxygen to the coal surface so an ignition occurred. In perspective of safety management in industrial sites, spraying with appropriate concentration of $CaCl_2$ to the deposited coal dust according to the surface temperature of the equipment can improve the MAIT of the dust, corresponding it could reduce the risk of fire and explosion.

3.6. Decomposition of $CaCl_2$ treated coal samples in air

According to the MAIT results in section 3.5, the coal sample treated with 200 g/L calcium chloride solution had the best inhibition effect on the ignition risk from both in economy and technology. Therefore, the typical TGA-DSC curves of the 200 g/L $CaCl_2$-Coal sample heated under oxidative conditions was analysed and compared with the H_2O-Coal sample. Fig. 8 demonstrates the mass loss, mass loss rate, and heat release characteristics of the two samples at heating rate of 10 °C/min. Based upon previous studies on CSC process [7,40,41], the self-heating of the coal sample was classified into four stages, including moisture evaporation stage (I), oxygen chemisorption stage (II), combustion stage (III), and burnout stage (IV). To characterise the slow oxidation properties, basic parameters derived from TGA-DSC curves of the samples are summarised in Table 4.

The temperature at minimal mass of moisture evaporation ($T_{min\text{-}I}$), temperature at the maximum mass increase ($T_{max\text{-}II}$), mass loss (W_I) at $T_{min\text{-}I}$, and mass increases (W_{II}) at $T_{max\text{-}II}$ were showed in Fig. 8c. The heat evolution during oxygen chemisorption (ΔQ) was obtained by integration of DSC in the corresponding temperature interval [27]. Slovák [42] directly defined the heat released per gram of coal sample mass (Q_o) as Eqs. (2) and (3).

$$\Delta Q = \int_{t_{max-II}}^{t_{min-I}} q\,dt = \frac{\Delta S}{\beta} \tag{2}$$

$$Q_o = \frac{\Delta Q}{W} \cdot 100 \tag{3}$$

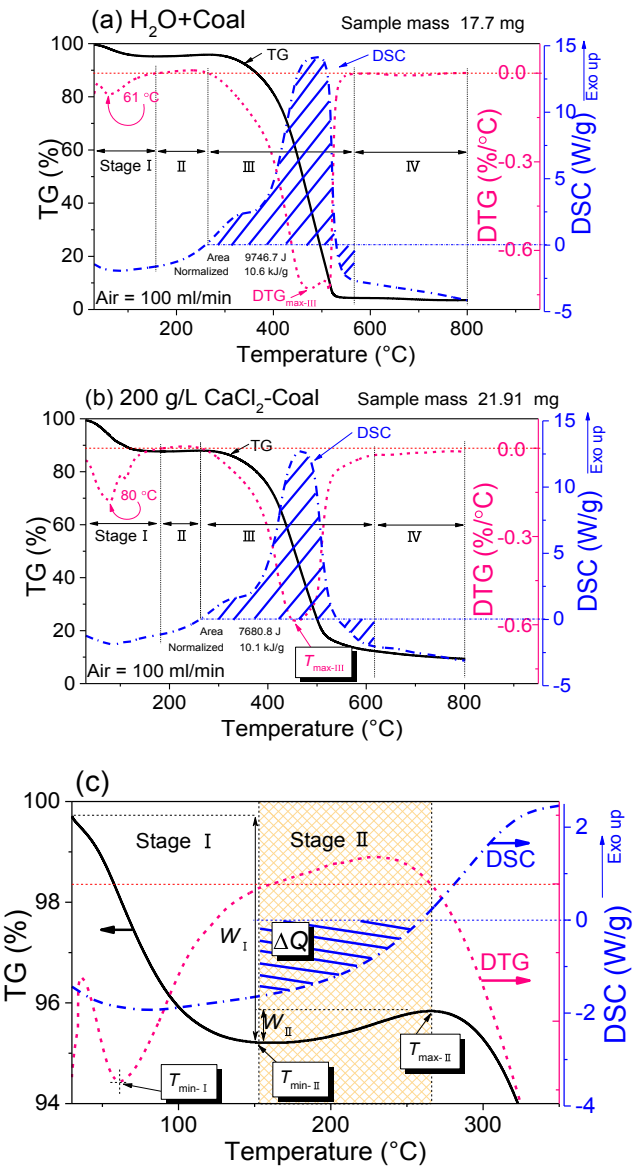

Fig. 8. TGA-DSC results of the coal samples before and after resistant treatment at heating rate of 10 °C/min, (a) H_2O-Coal sample, (b) 200 g/L $CaCl_2$-Coal sample, (c) parameters derived from TG, DTG, and DSC curves (W_I (%) is the weight loss at the minimal mass of moisture evaporation in stage I, W_{II} (%) is the maximum mass increase in stage II).

where ΔQ is the sum of the heat released from coal at corresponding stage, kJ/g, ΔS is the area obtained by integration of DSC in the temperature interval, J, q is the heat flow per gram of sample, W/g, t is the time, s, $t_{min\text{-}I}$ and $t_{max\text{-}II}$ are the time corresponding to the temperature of $T_{min\text{-}I}$ and $T_{max\text{-}II}$, s, β is the heating rate, °C/min.

3.6.1. Stage I

Both samples were died to evaporate moisture under the same thermal conditions at the initial heating process of stage I. As shown in Fig. 8a and b, the mass of 200 g/L $CaCl_2$-Coal decreased from the initial of heating up to about 183 °C, which had a wide humidity loss interval than that of H_2O-Coal sample (from ambient to about 157 °C). Calcium chloride can form several hydrates due to its highly hygroscopic properties at ordinary temperatures. According to the calcium chloride handbook from the Doe Chemical Company [43], there are four solid hydrates of calcium chloride (hexa-, tetra-, di-, and monohydrate) which have been identified in a calcium chloride-water system. The possible

Table 4
Effects of $CaCl_2$ on the decomposition parameters during oxidation process of coal in air at heating rate of 10 °C/min.

Sample	Stage	Temp. range (°C)	Mass loss (%)	$T_{min\text{-}I}$ (°C)	$DTG_{min\text{-}I}$ (%/°C)	$T_{min\text{-}II}$ (°C)	$T_{max\text{-}III}$ (°C)	$DTG_{max\text{-}III}$ (%/°C)	Residue (%)
H_2O-Coal	I	30–157	−4.79	61	–0.07	265	457	–0.73	3.53
	II	157–265	0.63						
	III	265–567	−91.48						
	IV	567–800	−0.87						
200 g/L $CaCl_2$-Coal	I	30–183	−12.33	80	–0.18	263	473	–0.58	9.36
	II	183–263	0.3						
	III	263–616	−75.66						
	IV	616–800	−2.95						

Notes: $T_{min\text{-}I}$, temperature at minimal mass of moisture evaporation in stage I,°C; $T_{max\text{-}II}$, temperature at the maximum mass loss in stage II,°C; $T_{max\text{-}III}$, temperature at the maximum mass loss rate in stage III, °C; $DTG_{min\text{-}I}$, peak mass loss rate in stage I, (%/°C); $DTG_{max\text{-}III}$, peak mass loss rate in stage III, (%/°C).

decomposition pathway of the hydrates may occur under the following conditions as Eqs. (4) to (7) [43,44].

$$CaCl_2{\cdot}6H_2O(s) \rightarrow CaCl_2{\cdot}4H_2O(s) + 2H_2O(s, l)\ –55–30\ °C \quad (4)$$

$$CaCl_2{\cdot}4H_2O(s) \rightarrow CaCl_2{\cdot}2H_2O(s) + 2H_2O(s, l)\ 30–45\ °C \quad (5)$$

$$CaCl_2{\cdot}2H_2O(s) \rightarrow CaCl_2{\cdot}H_2O(s) + 2H_2O(l, g)\ 45–176\ °C \quad (6)$$

$$CaCl_2{\cdot}H_2O(s) \rightarrow CaCl_2(s) + H_2O(g)\ 176–260\ °C \quad (7)$$

The coal sample treated with $CaCl_2$ lost more moisture during the decomposition of the hydrates than that of the blank coal sample. Therefore, it is obvious that the mass loss of 200 g/L $CaCl_2$-treated Coal (12.33%) at stage I was 2.5 times than that of H_2O-Coal sample (4.79%) (Table 4). The maximum mass loss rate of the 200 g/L $CaCl_2$-Coal and H_2O-Coal samples at stage I was 0.18 and 0.07%/°C at the correspondingly temperature ($T_{min\text{-}I}$) of 80 and 61 °C, respectively. Increasingly, the emerge of the temperature point (80 °C) of the $CaCl_2$-Coal sample at the maximum mass loss rate in this stage was consistent with the appearance of the first maximum inhibiting rate point (around 81.7 °C) from hot plate test (Fig. 6). It is understandable that more moisture evaporation of the $CaCl_2$-treated Coal sample takes more heat away, resulting in a slower temperature rise rate in the initial of self-heating under the same thermal environment.

3.6.2. Stage II

The increase of coal sample mass (in stage II) was ascribed to oxygen chemisorption. The carbonaceous matter on coal surface reacted with oxygen in this stage to form surface oxygen containing species (ethers, carbonyls, carboxyles) [45]. The mass of the 200 g/L $CaCl_2$-treated coal sample increased by 0.3% within the temperature range of 183 to 263 °C. However, the mass of H_2O-Coal sample increased by 0.64% was about 2 times more than that of $CaCl_2$-Coal sample (0.3%) at the same conditions (Table 4). This is due to the fact that the coal surface covered by the inorganic solids film acted as a wall which reduced the gas-phase oxidation of hydrocarbons from volatile combustibles (Fig. 4e–f), preventing the formation of coal-oxygen interactions. Generally, the oxygen chemisorption on the surface of coal char accompanied with the physical adsorption was an exothermic process [46]. However, an opposite trend was observed that both samples in this stage (below $T_{max\text{-}II}$) exhibited endothermic characteristics. Based on Eqs. (2) and (3), the $Q_{o\text{-}II}$ of $CaCl_2$-treated coal (–106.3 kJ/g) absorbed more heat than that of H_2O-treated coal (–98.4 kJ/g), indicating that per unit 200 g/L $CaCl_2$-Coal sample has higher endothermic capacity at this slow oxidation phase. This was supported by Eq. (7) that the heat absorbed by $CaCl_2$-Coal sample at stage II was from the decomposition of calcium chloride monohydrate dehydration. A DSC analysis by Pandey et al. [17] confirmed that a normalised value of –1653.09 J/gm was estimated by 0.5 mg of $CaCl_2$ at the temperature range from 43.96 to 252.38 °C. On the other hand, the intermediate products of coal-oxygen interactions were not always formed by exothermal reactions because the amount and the nature of the intermediate products were sensitive to the experimental conditions, especially in TGA-DSC curves. Marinov's explanation about the interaction of coal with oxygen in his experiment [47] suggested that the changes in weight and the oxygen chemisorption was related to the composition of the gas phase and on the concentration of moisture vapour in the pore volume. An endothermicity of the thermo-oxidative degradation of brown coal was observed at temperature from 100 to 280 °C. In addition, another test of lignite showed the proceeding of an endothermal process at the DTA curve above 165 °C. These findings are consistent with our results in present work.

3.6.3. Stage III

Combustion stage III is the main mass loss phase of the sample due to pyrolysis and combustion of carbonaceous component. A weight loss of 75.66% for 200 g/L $CaCl_2$-Coal sample was lower than H_2O-Coal sample of 91.48%. The $DTG_{max\text{-}III}$ of $CaCl_2$-Coal sample (0.58%/°C) was lower than that of H_2O-Coal sample (0.73%/°C), indicating that treatment of $CaCl_2$ to the coal slowed down its reaction rate at this stage. With an addition of $CaCl_2$ to coal sample, the main temperature zone of stage III for 200 g/L $CaCl_2$-Coal sample (from 263 °C to 616 °C) had been enlarged about 51 °C in comparison to H_2O-Coal sample (from 265 °C to 567 °C) (Table 4). These results were consistence with Wang et al.'s findings [19] about $CaCl_2$ on reducing the combustion rate and expanding the main combustion zone of coal. According to literatures [43,44,48], the following reactions may occur with presence of water vapour in the atmosphere when the temperature was above 260 °C.

$$CaCl_2(s) + H_2O(g) \rightarrow Ca(OH)Cl(s) + HCl(g)\ 410–740\ °C \quad (8)$$

$$2Ca(OH)Cl(s) \rightarrow CaO{\cdot}CaCl_2(s) + H_2O(g)\ 479–564\ °C \quad (9)$$

$$Ca(OH)Cl(s) + CO_2(g) \rightarrow CaCO_3(s) + HCl(g)\ 410–640\ °C \quad (10)$$

Reactions (8) to (10) indicated that the intermediate reaction product calcium hydroxychlorie (Ca(OH)Cl) may be yield from anhydrous calcium chloride in an atmosphere with presence of water vapour, carbon dioxide, and oxygen above 410 °C. On the basis of a TG-DSC experiment, Allal et al. [48] stated that the dehydration of Ca(OH)Cl was an endothermic process at a temperature range from 479 to 564 °C with a value of reaction enthalpy about 23.718 kcal/mol. This was agreement with our results that the $Q_{o\text{-}III}$ of 200 g/L $CaCl_2$-Coal sample (10.1 kJ/g) was slightly lower than that of H_2O-Coal sample (10.6 kJ/g), indicating that $CaCl_2$ had effect on reducing the thermal release of coal.

3.6.4. Stage IV

The mass of 200 g/L $CaCl_2$-Coal sample at the final temperature interval from 616 to 800 °C lost about 2.95%, while the H_2O-Coal sample reduced a little of 0.87% of its mass in this stage. It indicated that $CaCl_2$-Coal sample at stage IV still maintained a certain chain combustion reaction to promote slow decomposition of coal. Higher residue of $CaCl_2$ treated coal at the final decomposition phase was 9.36% which mainly attributed to unfired char and ash. At stage IV, the possible pathways of $CaCl_2$ may be occurred as following [44].

$$CaCl_2(s) + 0.5O_2(g) \rightarrow CaO(s) + Cl_2(g)\ 600–800\ °C \quad (11)$$

$$CaCl_2(g) + CO_2(g) + 0.5O_2(g) \rightarrow CaCO_3(s) + Cl_2(g) > 782\ ^\circ C \quad (12)$$

Reactions (11) and (12) indicated that calcium oxide and calcium carbonate may produced at this stage which may participate in the combustion chain reaction of coal sample.

3.7. Inspiration of $CaCl_2$ application on spontaneous coal combustion

Fig. 9 shows the mechanism of calcium chloride on the self-ignition of coal dust accumulation. Both physical and chemical effects of $CaCl_2$ on the process of coal combustion existed simultaneously. A comparison of the TGA-DSC results of the samples in tests at heating rate of 10 °C/min (Fig. 8 and Table 4) indicated that the coal treated with $CaCl_2$ could lengthen the moisture evaporation stage and reduce the oxygen chemisorption capacity at low-medium temperature, suggesting an obvious suppressing potential in self-ignition risk of coal by means of heat absorption during water evaporation process. This was supported by Eq. (7) that the dehydration of the $CaCl_2{\cdot}H_2O$(s) showed endothermic characteristic at the corresponding temperature interval. The addition of the calcium chloride hydrate to a coal accumulation absorbed the heat released from the coal-oxygen reactions during self-heating process, thus the endothermic characteristics of $CaCl_2$ acted as a heat sink within 263 °C for 200 g/L $CaCl_2$-Coal sample. Furthermore, the inorganic solids (Fig. 3e–f) on the covered surface aggravated the diffusion difficulty of oxygen molecules in contaction with the reactive active sites on the surface of coal surface. This was also the reason that the addition of the $CaCl_2$ reduced the oxidation reaction rate through starvation and therefore reduced the self-ignition risk of coal (Fig. S1c).

At medium lever of thermal condition (300–600 °C), the addition of $CaCl_2$ to coal sample reduced the decomposition reaction rate of coal but expanded the main combustion zone. This may be caused by dehydration or intermediate products (Ca(OH)Cl) decomposition of calcium chloride hydrate of which the endothermic processes reduced the combustion intensity of coal to a certain extent. However, the temperature evolution of $CaCl_2$ treated coal accumulation after the crossing point based upon hot plate test exhibited catalytic effect for coal smouldering combustion because the sample had higher temperature (Fig. 5c). This is because that the pulverized coal dust layer on hot surface in air is an open and heterogeneous combustion condition. The pulverized coal particles in the accumulation layer was not ignited and burnt at the same time, but first ignited at some priority sensitive parts [25] and then triggered the ignition at other parts of the layer successively [49]. After the ignition point was generated, it then moved towards the part with sufficient oxygen supply. In addition, when the temperature belonged 600 °C, the involved chemical effect of the $CaCl_2$ on coal combustion were through the following pathway [22,50]:

$$2CaO + O_2 \rightarrow 2CaO_2 \quad (13)$$

$$2CaO_2 + C \rightarrow CO_2 + 2CaO \quad (14)$$

Eqs. (13) and (14) suggested that the oxygen may be transported to the carbon surface by calcium oxide to participate in the coal-oxygen interactions. From XRD result of the $CaCl_2$-treated Coal sample in Fig. S2, the peak position at $2\theta = 26.7^\circ$ (CaO; PDF no. 28–0775) was attributed to calcium oxide (CaO; PDF no. 28–0775). The amplitude of the CaO peak at the heating stage of T_2 was 1.1 times than that at the stage of T_1, which confirmed that the calcium oxide was involved in the smoldering combustion and its yield increased after the thermal runaway occurred. The constituent Ca^{2+} in the form of its oxides (CaO and CaO_2) involved in the combustion reaction and lengthened the chain reaction paths. It promoted the decomposition of coal at high

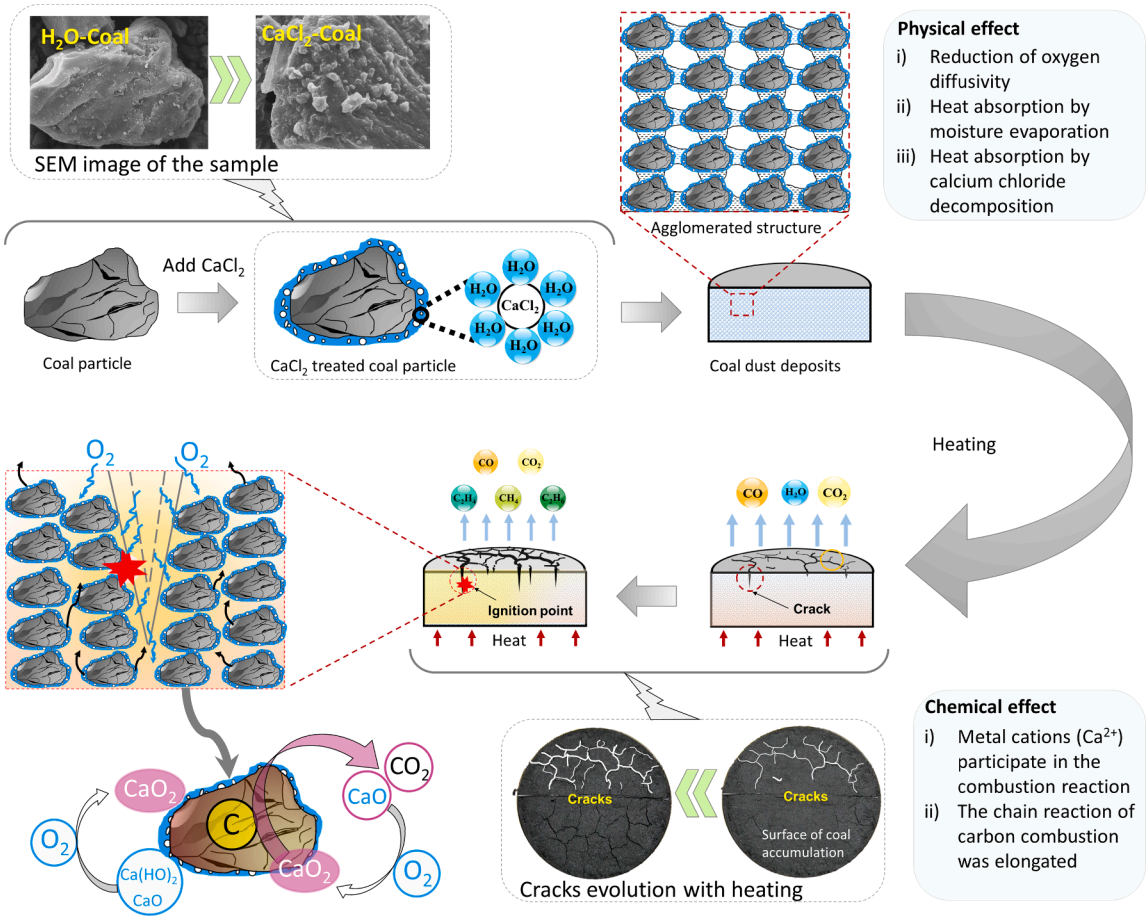

Fig. 9. Mechanism of $CaCl_2$ on the oxidation reactivity of coal dust accumulation.

thermal condition. Therefore, the temperature of the $CaCl_2$-Coal sample accumulation layer remained at a high level after the crossing point at the later duration of hot plate test.

4. Conclusions

For coal sample treated with calcium chloride, the minimum auto-ignition temperature (MAIT) of the sample was increased from 210 to 240 °C, with a max increasing temperature of 30 °C in comparison to H_2O-Coal sample. The evidences confirmed the inhibition effect of $CaCl_2$ on the thermal runaway during self-ignition process of the coal accumulation at low thermal conditions (before crossing point). In consideration of the corrosion of chlorine salts, the optimal suppression concentration of calcium chloride in present study is 200 g/L. However, results also found that the $CaCl_2$ promoted the decomposition of coal at high thermal conditions (after crossing point) in ambient. For 50 g/L $CaCl_2$-Coal sample on hot surface of 240 °C, the calculated inhibiting rate at 10 and 50 min was 54.8% and –115.6%, respectively, suggesting that the catalysis effect at the later stage after ignition was over two times than the inhibiting effect at the initial self-ignition process. This was attributed to the constituent calcium in the form of its oxides (CaO and CaO_2) which participated in the coal-oxygen complex reactions, so the addition of $CaCl_2$ in the combustion reaction lengthened the chain reaction paths and played a catalytic role in the coal combustion. For safety management of industrial sites involving coal dust, spraying $CaCl_2$ solution to coal could extend the ignition delay time of the coal dust layer. To some extent, it could prevent coal fire or explosion from getting out control of thermal runaway.

CRediT authorship contribution statement

Bei Li: Conceptualisation, Methodology, Formal analysis, Investigation, and Writing - original draft. **Hong - peng Lv:** Investigation, Data curation. **Jun Deng:** Resources, Writing - review & editing. **Li - li Ye:** Validation and Data curation. **Wei Gao:** Investigation and Project administration; Min-Shu Bi: Investigation and Supervision.

Declaration of Competing Interest

The authors declare that they have no known competing financial interests or personal relationships that could have appeared to influence the work reported in this paper.

Acknowledgments

The research was supported by the National Natural Science Foundation of China (No. 51904054), the Fundamental Research Funds for the Central Universities of China (Nos. DUT21JC14, DUT20RC(3)015, and DUT2020TB03), and the Open Projects of State Key Laboratory of Coal Resources in Western China (No. SKLCRKF20-02).

Appendix A. Supplementary data

Supplementary data to this article can be found online at https://doi.org/10.1016/j.fuel.2021.121451.

References

[1] Heffern EL, Coates DA. Geologic history of natural coal-bed fires, Powder River basin, USA. Int J Coal Geol 2004;59(1-2):25–47.
[2] Engle MA, Radke LF, Heffern EL, O'Keefe JMK, Hower JC, Smeltzer CD, et al. Gas emissions, minerals, and tars associated with three coal fires, Powder River Basin, USA. Sci Total Environ 2012;420:146–59.
[3] Syed TH, Riyas MJ, Kuenzer C. Remote sensing of coal fires in India: A review. Earth-Sci Rev 2018;187:338–55.
[4] Liang Y, Liang H, Zhu S. Mercury emission from coal seam fire at Wuda, Inner Mongolia, China. Atmos Environ 2014;83:176–84.
[5] Kuenzer C, Stracher GB. Geomorphology of coal seam fires. Geomorphology 2012; 138(1):209–22.
[6] Singh A, Raju A, Pati P, Kumar N. Mapping of coal fire in Jharia Coalfield, India: a remote sensing based approach. J Indian Soc Remote 2017;45(2):369–76.
[7] Song J-J, Deng J, Zhao J-Y, Zhang Y-N, Shu C-M. Comparative analysis of exothermic behaviour of fresh and weathered coal during low-temperature oxidation. Fuel 2021;289:119942. https://doi.org/10.1016/j.fuel.2020.119942.
[8] Shan B, Wang G, Cao F, Wu D, Liang WX, Sun RY. Mercury emission from underground coal fires in the mining goaf of the Wuda Coalfield. China. Ecotox Environ Safe 2019;182:109–409.
[9] Li J, Li Z, Yang Y, Kong B, Wang C. Laboratory study on the inhibitory effect of free radical scavenger on coal spontaneous combustion. Fuel Process Technol 2018; 171:350–60.
[10] Meng X, Liu Q, Luo X, Zhou X. Risk assessment of the unsafe behaviours of humans in fatal gas explosion accidents in China's underground coal mines. J Clean Prod 2019;210:970–6.
[11] Li J-L, Lu W, Cao Y-J, Kong B, Zhang Q-S. Method of pre-oxidation treatment for spontaneous combustion inhibition and its application. Process Saf Environ Prot 2019;131:169–77.
[12] Wu Z, Hu S, Jiang S, He X, Shao H, Wang K, et al. Experimental study on prevention and control of coal spontaneous combustion with heat control inhibitor. J Loss Prev Process Ind 2018;56:272–7.
[13] Yang Y, Tsai YT, Zhang YN, Shu CM, Deng J. Inhibition of spontaneous combustion for different metamorphic degrees of coal using Zn/Ma/Al-CO_3 layered double hydroxides. Process Saf Environ Prot 2018;113:401–12.
[14] Guo J, Cai GB, Jin Y, Zheng XZ, Liu Y. An improved composite fly ash gel to extinguish underground coal fire in close distance coal seams: a case study. Adv Mater Sci Eng 2020;6:5695471.
[15] Zhai X, Wu S, Wang K, Drebenstedt C, Zhao J. Environment influences and extinguish technology of spontaneous combustion of coal gangue heap of Baijigou coal mine in China. Energy Procedia 2017;136:66–72.
[16] Wang XD. Research on technical measures of fire prevention and extinguishing in mine. Energy Energy Conserv 2020;04:136–7 (in Chinese).
[17] Pandey J, Mohalik NK, Mishra RK, Khalkho A, Kumar D, Singh VK. Investigation of the role of fire retardants in preventing spontaneous heating of coal and controlling coal mine fires. Fire Thechnol 2015;51(2):227–45.
[18] Tang Y-B, Li Z-H, Yang YI, Ma D-J, Ji H-J. Effect of inorganic chloride on spontaneous combustion of coal. J South Afr Inst Min Metall 2015;115(2):87–92.
[19] Wang H, Dlugogorski BZ, Kennedy EM. Pathways for production of CO_2 and CO in low-temperature oxidation of coal. Energy Fuel 2003;17(1):150–8.
[20] Cui C, Jiang S, Shao H, Zhang W, Wang K, Wu Z. Experimental study on thermo-responsive inhibitors inhibiting coal spontaneous combustion. Fuel Process Technol 2018;175:113–22.
[21] Wang C, Zhao L, Yuan M, Du Y, Zhu C, Liu Y, et al. Effects of minerals containing sodium, calcium, and iron on oxy-fuel combustion reactivity and kinetics of Zhundong coal via synthetic coal. J Therm Anal Calorim 2020;139(1):261–71.
[22] Pan WP. Effect of calcium of calcium chloride and calcium acetate on the reactivity of a lignite coal at low heating rate. Thermochim Acta 1988;125:285–94.
[23] Sunel K, He Y, Wang ZH, Liu LL, Zhu YQ, Cen KF. Metal chloride influence on syngas component during coal pyrolysis in fixed-bed and entrained flow drop-tube furnace. Sci China-Technol Sci 2019;62(11):2029–37.
[24] Wu D, Huang X, Norman F, Verplaetsen F, Berghmans J, Van den Bulck E. Experimental investigation on the self-ignition behaviour of coal dust accumulations in oxy-fuel combustion system. Fuel 2015;160:245–54.
[25] Li B, Li M, Gao W, Bi M, Ma Li, Qin Q, et al. Effects of particle size on the self-ignition behaviour of a coal dust layer on a hot plate. Fuel 2020;260:116269. https://doi.org/10.1016/j.fuel.2019.116269.
[26] Zhong X, Qin B, Dou G, Xia C, Wang F. A chelated calcium-procyanidine-attapulgite composite inhibitor for the suppression of coal oxidation. Fuel 2018; 217:680–8.
[27] Slovák V, Taraba B. Urea and $CaCl_2$ as inhibitors of coal low-temperature oxidation. J Therm Anal Calorim 2012;110(1):363–7.
[28] Smith AC, Miron Y, Lazzara CP. Inhibition of spontaneous combustion of coal. Report of Investigations, Bureau of Mines, United States Department of the Interior 1988;9196:285–294.
[29] Lu J-J, Chen W-H. Investigation on the ignition and burnout temperatures of bamboo and sugarcane bagasse by thermogravimetric analysis. Appl Energ 2015; 160:49–57.
[30] Rice GS, Greenwald HP. Coal-dust explosibility factors indicated by experimental mine investigations 1911 to 1929. USBM Tech Paper 1929;464:45.
[31] Sapko MJ, Cashdollar KL, Green GM. Coal dust particle size survey of US mines. J Loss Prev Process Ind 2007;20(4-6):616–20.
[32] Joshi KA, Raghavan V, Rangwala AS. An experimental study of coal dust ignition in wedge shaped hot plate configurations. Combust Flame 2012;159(1):376–84.
[33] Li B, Liu G, Bi M-S, Li Z-B, Han B, Shu C-M. Self-ignition risk classification for coal dust layers of three coal types on a hot surface. Energy 2021;216:119197. https://doi.org/10.1016/j.energy.2020.119197.
[34] Wu D, Song Z, Schmidt M, Zhang Qi, Qian X. Theoretical and numerical study on ignition behaviour of coal dust layers on a hot surface with corrected kinetic parameters. J Hazard Mater 2019;368:156–62.
[35] Miao M, Deng B, Kong H, Yang H, Lyu J, Jiang X, et al. Effects of volatile matter and oxygen concentration on combustion characteristics of coal in an oxygen-enriched fluidized bed. Energy 2021;220:119778. https://doi.org/10.1016/j.energy.2021.119778.

[36] Wang C, Wang C, Jia X, Gao X, Wang P, Feng Q, et al. Experimental investigation on combustion characteristics and kinetics during Co-Firing bituminous coal with ultra-low volatile carbon-based solid fuels. J Energy Inst 2021;95:87–100.
[37] Otake Y, Walker PL. Pyrolysis of demineralized and metal cation loaded lignites. Fuel 1993;72(2):139–49.
[38] Maes II, Gryglewicz G, Yperman J, Franco DV, Mullens J, Van Poucke LC. Effect of calcium and calcium minerals in coal on its thermal analysis. Fuel 1997;76(2):143–7.
[39] Clemens AH, Damiano LF, Matheson TW. The effect of calcium on the rate and products of steam gasification of char from low rank coal. Fuel 1998;77(9-10):1017–20.
[40] Qi X, Li Q, Zhang H, Xin H. Thermodynamic characteristics of coal reaction under low oxygen concentration conditions. J Energy Inst 2017;90(4):544–55.
[41] Li B, Liu G, Gao W, Cong H-Y, Bi M-S, Ma Li, et al. Study of combustion behaviour and kinetics modelling of Chinese Gongwusu coal gangue: Model-fitting and model-free approaches. Fuel 2020;268:117284. https://doi.org/10.1016/j.fuel.2020.117284.
[42] Slovák V, Taraba B. Effect of experimental conditions on parameters derived from TG–DSC measurements of low-temperature oxidation of coal. J Therm Anal Calorim 2010;101(2):641–6.
[43] Company TDC. Calcium chloride handbook: a guide to properties, forms, storage and handling. Midland, USA: The Doe Chemical Company Customer Information Center; 2003.
[44] Fraissler G, Jöller M, Brunner T, Obernberger I. Influence of dry and humid gaseous atmosphere on the thermal decomposition of calcium chloride and its impact on the remove of heavy metals by chlorination. Chem Eng Process 2009;48(1):380–8.
[45] Wang H, Dlugogorski BZ, Kennedy EM. Coal oxidation at low temperatures: Oxygen consumption, oxidation products, reaction mechanism and kinetic modeling. Prog Energy Combust Sci 2003;29:487–513.
[46] Yuan H, Richter F, Rein G. A multi-step reaction scheme to simulate self-heating ignition of coal: Effects of oxygen adsorption and smouldering combustion. Proce Combust Inst 2021;38(3):4717–25.
[47] Marinov VN. Self-ignition and mechanisms of interaction of coal with oxygen at low temperatures. 2. Changes in weight and thermal effects on gradual heating of coal in air in the range 20–300 °C. Fuel 1977;56(2):158–64.
[48] Allal KM, Dolignier JC, Martin G. Reaction mechanism of calcium hydroxide with gaseous hydrogen chloride. Revue de ITFP 1998;53(6):871–80.
[49] Yuan CM, Huang DZ, Li C, Li G. Ignition behaviour of magnesium powder layers on a plate heated at constant temperature. J Hazard Mater 2013;246–247:283–90.
[50] Cheng J, Zhou F, Xuan X, Liu J, Zhou J, Cen K. Cascade chain catalysis of coal combustion by Na–Fe–Ca composite promoters from industrial wastes. Fuel 2016;181:820–6.